Available online at www.sciencedirect.com
ScienceDirect
Journal of Sound and Vibration 318 (2008) 506–526
JOURNAL OF SOUND AND VIBRATION
www.elsevier.com/locate/jsvi

Dynamic viscoelastic effects on sound wave scattering by an eccentric compound circular cylinder

Seyyed M. Hasheminejad*, Siavash Kazemirad

Acoustics Research Laboratory, Department of Mechanical Engineering, Iran University of Science and Technology, Narmak, Tehran 16844, Iran

Received 19 August 2007; received in revised form 9 April 2008; accepted 15 April 2008
Handling Editor: A.V. Metrikine
Available online 2 June 2008

Abstract

The classical method of separation of variables in conjunction with the translational addition theorem for cylindrical wave functions are employed to obtain an exact solution for two-dimensional interaction of a harmonic plane acoustic wave with an infinitely long (visco)elastic circular cylinder which is eccentrically coated by another (visco)elastic material and is submerged in an ideal unbounded acoustic medium. The novel features of Havriliak–Negami model for dynamic viscoelastic material behaviour are used to take the rheological properties of the coating (and/or core) material into consideration. The analytical results are illustrated with numerical examples in which a steel rod eccentrically coated with (an eccentric steel shell filled with) dissipative materials of distinct viscoelastic properties is insonified by plane sound waves at selected angles of incidence. The effects of incident wave frequency, angle of incidence, core eccentricity and dynamic viscoelastic material properties on the backscattered form function spectra are examined. Limiting cases are considered and fair agreements with available solutions are obtained.

1. Introduction

Numerous researchers have investigated the problem of acoustic scattering from coated obstacles submerged in an unbounded fluid medium. In particular, the problem of the interaction of acoustic waves with fluid-loaded cylinders and cylindrical shells with an external compliant layer has long been of practical interest. For example, Junger and Garrelick [1] applied a Kirchhoff-type formulation to compute the backscattering cross sections of rigid cylinders covered with partial coatings of arbitrary impedance. Gaunaurd [2,3] used the approach developed by Doolittle and Uberall [4] in conjunction with the Kelvin–Voigt viscoelastic model to solve the problem of an infinite hollow elastic cylinder covered with an ideal layer of viscoelastic material. Neubauer [5] utilized results of the classical solution to the problem of reflection by a two-layer cylindrical shell for the determination of the material properties of a reflection-reduction coating, including inherent wave attenuation effects in both layers. Flax and Neubauer [6] developed

*Corresponding author. Tel.: +98 21 73912957; fax: +98 21 22549196.
E-mail address: hashemi@iust.ac.ir (S.M. Hasheminejad).

0022-460X/$ - see front matter © 2008 Elsevier Ltd. All rights reserved.
doi:10.1016/j.jsv.2008.04.022

a mathematical model to predict the wave pattern resulting from a plane acoustic wave scattered by a two-layered absorptive cylindrical shell with different fluid media inside and outside. Poruchikov and Stepanov [7] examined the effect of acoustic waves on a rigid immobile infinite cylinder covered with a thin compressible coating and immersed in an unbounded fluid. Ayres and Gaunaurd [8] studied the acoustic wave scattering from a hollow elastic cylinder covered with a viscoelastic coating, and calculated the mode shapes of the resonances in the low-frequency range. Sinai and Waag [9] computed the scattered pressure field from a fluid-loaded two-layered cylinder for a range of frequencies, material parameters, and emitter and detector functions. Adamova and Kanibolotskii [10] analysed the problem of the optimal design of a cylindrically laminar sound-reflecting shield for minimal sound transmission into a multilayered fluid-filled infinite cylinder subjected to a plane harmonic wave of unit amplitude perpendicular to the axis of the cylinder. Ferri et al. [11] addressed the scattering of acoustic plane waves from submerged cylinders that are partially covered with a compliant (pressure-release) coating. Sinclair and Addison [12] developed the equations of the scattering of a plane acoustic/elastic wave from a two-layered cylinder embedded in a solid or a fluid medium. Laulagnet and Guyader [13] used asymptotic expansions to present the mathematical analysis and numerical results for the vibroacoustic behaviour of a coated finite cylindrical shell. Laulagnet and Guyader [14] subsequently considered acoustic radiation from partially coated finite shells and developed results for the total radiated acoustic power and the surface average velocity response. Partridge [15] applied the deformed cylinder method (DCM) to study acoustic scattering from elastic bodies (shells) that are covered to varying degrees by a viscoelastic absorbing layer. Honarvar and Sinclair [16] developed a detailed formulation for the scattering of an obliquely incident plane acoustic wave from a submerged clad rod. They calculated the effects of variations in the cladding thickness on both the backscattered pressure spectrum and individual normal modes of vibration. Ginsberg [17] considered the two-dimensional problem of scattering of a plane wave incident on an infinite cylinder that is partially coated with strips of pressure-release material and presented a quantitative analysis of the global effect on acoustic scattering of viscosity effects. Cuschieri and Feit [18] examined the influence of a partial coating by a normally reacting (impedance) layer on the acoustic radiation from a fluid-loaded, cylindrical shell of infinite extent and excited by either a line force or an incident plane acoustic wave. Luo et al. [19] used the Donnell shell theory to present an analysis of sound radiation from a ring-stiffened cylindrical shell coated with a viscoelastic layer. Fan et al. [20] assessed a resonance acoustic spectroscopy technique for non-destructive evaluation of explosively welded clad rods, modelled as two-layered cylinders with a spring–mass system to represent a thin interfacial layer containing the weld. Hasheminejad and Safari [21] presented a rigorous analysis and numerical results for scattering of acoustic waves from a viscoelastically coated cylinder submerged in a viscous fluid medium. Ivanov [22] investigated the direct and inverse problems of plane wave diffraction by a circular cylinder with a perforated coating. He selected the parameters of the perforated coating so as to ensure a given level of suppression for the field diffracted by the cylinder in the context of the inverse problem. Mitri [23] developed theoretical analysis for the acoustic radiation force due to incident plane progressive waves on elastic cylindrical shells covered with a layer of viscoelastic material. He performed numerical calculations of the radiation force function for stainless steel cylindrical shells coated by a phenolic polymer-type material and examined the effect of sound absorption by the viscoelastic layer. Cuschieri [24] considered scattering and radiation of acoustic waves from a fluid-loaded infinite cylindrical shell with an external compliant layer, and established the consistency between the scattering results from the normally reacting impedance layer model of zero thickness to those from the multilayer shell model. In a closely related problem, Barshinger and Rose [25] investigated the propagation of ultrasonic guided waves in an elastic hollow cylinder with a viscoelastic coating, with application in non-destructive inspection of viscoelastically coated piping and tubing.

Analytical solutions of interior or exterior boundary value problems in various fields such as potential theory, acoustics and electromagnetism, are strictly dependent on the shape of boundaries. In particular, when multiple interfaces are present in a wave field, there is an interaction between them due to cross scattering. Several researchers have studied the wave interaction problems involving eccentric cylindrical boundaries. Most of these researchers have utilized classical separation of variables techniques in conjunction with translational addition theorems for cylindrical wave functions. Roumeliotis et al. [26] was perhaps the first who solved the problem of scattering of electromagnetic waves from an eccentrically coated infinite metallic cylinder. Shen [27] analysed electromagnetic scattering from an imperfectly conducting cylinder embedded in a

non-concentric chiroplasma cylinder. Morse et al. [28] showed that acoustic scattering by a non-concentric circular cylinder exhibits scattering processes not present in the simple case of uniform thickness. Roumeliotis and Kakogiannos [29] treated the scattering of a plane acoustic wave normal to the axis of an infinite impenetrable or penetrable cylinder of acoustically small radius, eccentrically coated by a penetrable cylinder. Danila et al. [30,31] used the generalized Debye series expansion (GDSE) method for calculation of the scattered field due to a plane wave incident on concentric or eccentric fluid–solid cylindrical interfaces. Roumeliotis and Savaidis [32] investigated the scattering of a plane electromagnetic wave by an infinite-circular dielectric cylinder, containing eccentrically an elliptic metallic one. Yin et al. [33] examined the multiple scattering from two infinitely long, parallel, non-overlapping circular impedance cylinders eccentrically coated with Faraday chiral media at normal incidence. Tanyer and Olsen [34] used perturbation theory to obtain a closed-form expression for the field produced by a plane wave incident on an infinitely long conducting cylinder, coated with a lossy dielectric of non-uniform thickness. Savaidis and Roumeliotis [35] treated the scattering of a plane electromagnetic wave by an infinite elliptic dielectric cylinder, coating eccentrically a circular metallic or dielectric inner cylinder. Yousif and Elsherbeni [36] presented the analytical solution for the scattering of electromagnetic plane waves from an infinitely long homogeneous cylinder of arbitrary material, in an eccentric coating at oblique incidence. Simao et al. [37] used the Debye series formalism to analyse the resonant scattering of light by a dielectric cylinder with an eccentric cylindrical metallic inclusion. Hasheminejad and Azarpeyvand [38] presented an exact analysis of acoustic radiation from a vibrating cylindrical source eccentrically suspended within a fluid cylinder. Savaidis and Roumeliotis [39] investigated scattering of a plane electromagnetic wave by an infinite-circular dielectric cylinder coating eccentrically an elliptic dielectric one. Hu et al. [40] developed an analytical technique, referred to as the scattering matrix method (SMM), to analyse the scattering of a planar wave from a conducting cylinder coated with non-uniform magnetized ferrite. Just recently, Mushref [41] developed series solution for electromagnetic (TM) wave scattering by an eccentrically coated circular cylinder in matrix form.

The above review clearly indicates that while there exists a notable body of literature on wave scattering from coated cylindrical obstacles, rigorous analytic or numerical solutions for sound wave scattering from a compound (visco)elastic cylinder with an eccentric core seem to be non-existent (see Fig. 1). Our primary goal is to fill this gap. Therefore, in this paper, we employ the novel features of Havriliak–Negami model for viscoelastic material behaviour, which is known to be among the most successful descriptions for the frequency dependence of the complex modulus of polymeric materials in the glass transition region [42,43], along with the translational addition theorem for cylindrical wave functions to formulate an exact analysis for the proposed problem. Attention is focused on the effects of core eccentricity as well as the dynamic

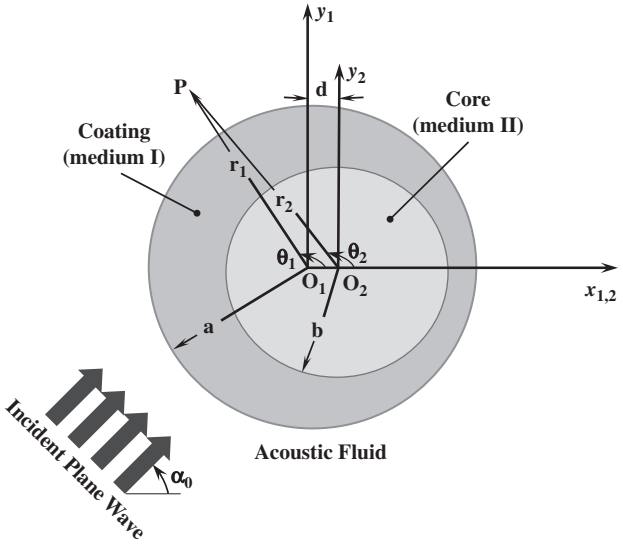

Fig. 1. Problem geometry.

viscoelastic material properties on the backscattering form function spectra. The proposed model is of interest essentially due to its inherent value as a canonical problem in structural acoustics. The presented exact solution can form an invaluable guide for assessment of effect of the coating non-uniformity (core eccentricity) on the scattered sound field of compound cylindrical components including viscoelastic materials. It is of important practical value in non-destructive characterization of clad rods or wires [20,44–50], cylindrical shells with dissipative fillings [51–53], coated optical fibers [54,55], and acoustic waveguides [56–59]. It can also serve as the benchmark for comparison to other solutions obtained by strictly numerical or asymptotic approaches.

2. Formulation

2.1. Acoustic field equations

Consider a plane compressional acoustic wave normally incident upon a compound cylinder defined by two non-concentric cylindrical surfaces of radii "a" and "*b*" immersed in an ideal boundless fluid medium. The problem geometry is shown in Fig. 1. Two polar coordinate systems $(r_i,\theta_i;\ i=1,2)$ are introduced to describe the different acoustic fields inside the coated cylinder. The cylinder axes extend to infinity and are parallel. Their origin-to-origin separation is d, and point P is an arbitrary field point outside the cylinder. The problem can be analysed by means of the standard methods of theoretical acoustics. Since the surrounding compressible medium is assumed to be inviscid and ideal (i.e., it cannot support shear stresses), the state of stress in the fluid is purely hydrostatic and the field equations may conveniently be expressed in terms of a scalar velocity potential as [60]

$$\mathbf{v}=\boldsymbol{\nabla}\varphi,\quad p=\mathrm{i}\omega\rho_0\varphi,\quad \nabla^2\varphi+k^2\varphi=0, \tag{1}$$

where $k=\omega/c_0$ is the wavenumber for the dilatational wave, ρ_0 is the fluid density, v is the fluid particle velocity vector, p is the acoustic pressure, c_0 is the speed of sound in the fluid, and in view of the fact that the incident wave is time-harmonic with the circular frequency ω, we have assumed harmonic time variations throughout with the $\mathrm{e}^{-\mathrm{i}\omega t}$ dependence suppressed for simplicity.

The dynamics of the problem may be expressed in terms of appropriate scalar potentials that can be represented in the form of an infinite generalized Fourier series whose unknown scattering coefficients are to be determined by imposing the proper boundary conditions. The incident wave in the cylindrical coordinate system of the outer cylinder (r_1,θ_1) may be written in the standard form [21]

$$\varphi_{\mathrm{inc.}}(r_1,\theta_1,\omega)=\varphi_0\sum_{n=-\infty}^{\infty}\mathrm{i}^n J_n(kr_1)\mathrm{e}^{\mathrm{i}n(\theta_1-\alpha_0)}, \tag{2}$$

where φ_0 is amplitude of the incident wave, α_0 is the angle of incidence, and J_n is the cylindrical Bessel function of the first kind [61]. Furthermore, the acoustic field scattered by the compound cylinder, is conveniently expressed in the form [21]

$$\varphi_{\mathrm{scat.}}(r_1,\theta_1,\omega)=\sum_{n=-\infty}^{\infty}A_n(\omega)H_n(kr_1)\,\mathrm{e}^{\mathrm{i}n\theta_1}, \tag{3}$$

where $A_n(\omega)$ is an unknown scattering coefficient, $H_n(x)=J_n(x)+\mathrm{i}\,Y_n(x)$ is the cylindrical Hankel function of order n [61]. Also, using Eq. (1), the radial velocity and pressure in the acoustic fluid are, respectively, written in terms of the total acoustic field potential $\varphi=\varphi_{\mathrm{inc.}}+\varphi_{\mathrm{scat.}}$ as

$$\mathrm{v}_r(r_1,\theta_1,\omega)=\frac{\partial\varphi}{\partial r}=k\varphi_0\sum_{n=-\infty}^{\infty}\mathrm{i}^n J_n'(kr_1)\mathrm{e}^{\mathrm{i}n(\theta_1-\alpha_0)}+k\sum_{n=-\infty}^{\infty}A_n(\omega)H_n'(kr_1)\mathrm{e}^{\mathrm{i}n\theta_1}, \tag{4a}$$

$$p(r_1,\theta_1,\omega)=\mathrm{i}\omega\rho_0\varphi=\omega\rho_0\varphi_0\sum_{n=-\infty}^{\infty}\mathrm{i}^{n+1}J_n(kr_1)\mathrm{e}^{\mathrm{i}n(\theta_1-\alpha_0)}+\mathrm{i}\omega\rho_0\sum_{n=-\infty}^{\infty}A_n(\omega)H_n(kr_1)\mathrm{e}^{\mathrm{i}n\theta_1}, \tag{4b}$$

where prime denotes differentiation with respect to the argument.

2.2. Viscoelastic field equations

Accurate mathematical modelling of materials manifesting quite definite rheological properties (e.g., viscoelastic damping materials) is difficult mainly because their measured dynamic properties are frequency and temperature dependent, and can also depend on the type of deformation and amplitude. Consequently, mathematical models describing the behaviour of viscoelastic materials cannot be clearly linked to the physical principles involved and thus empirical approaches are used. The most popular approach, called the structural damping model, uses complex constants as the material moduli. Strictly speaking, for viscoelastic and isotropic materials, two independent complex moduli are necessary for mechanical characterization; for example the complex Young's modulus $E^*(\omega) = E'(\omega) + iE''(\omega)$ and the complex shear modulus $G^*(\omega) = G'(\omega) + iG''(\omega)$. Both moduli, in principle, are frequency dependent. The main difficulty is the simultaneous presences of the Young's and shear complex moduli as well as the Poisson ratio. Practically, however, for viscoelastic isotropic materials the hypothesis of a constant (frequency-independent) and real Poisson ratio is often adopted [62].

The frequency dependent complex modulus $G^*(\omega) = G'(\omega) + iG''(\omega)$ of a polymer has several commonly observed characteristics: a rubbery plateau (G_0) at low frequencies, a glassy plateau at high frequencies (G_∞), and a rapidly changing modulus in the vicinity of the glass transition. The glass transition region is also characterized by a peak in the loss modulus (G'') and a peak in the loss factor, $\eta(\omega) = G''(\omega)/G'(\omega)$ (e.g., see Fig. 2). There have been several analytical models for this behaviour suggested in the literature with the most important expressions being the single relaxation time model of Cole-Cole [63], the Davidson–Cole method [64] which includes asymmetric frequency behaviour, and finally the Havriliak–Negami (HN) model [65] which includes aspects of the previous two models (i.e., it is a generalization of the single relaxation time model that combines both the broadening of the Cole–Cole model and the asymmetry of the Davidson–Cole model). Hartmann et al. [42] has shown that the H–N model can accurately describe the dynamic mechanical behaviour of polymers, including the height, width, position, and shape of the loss factor peak. Therefore, in the glass transition region, the real and imaginary parts of the complex shear modulus, $G^*(\omega)$ may advantageously be specified according to Havriliak–Negami model as [42]:

$$G'(\omega) = G_\infty + \frac{(G_0 - G_\infty)\cos(\beta\vartheta)}{[1 + 2\omega^\alpha\tau^\alpha\cos\gamma + \omega^{2\alpha}\tau^{2\alpha}]^{\beta/2}},$$
$$G''(\omega) = \frac{(G_\infty - G_0)\sin(\beta\vartheta)}{[1 + 2\omega^\alpha\tau^\alpha\cos\gamma + \omega^{2\alpha}\tau^{2\alpha}]^{\beta/2}}, \tag{5}$$

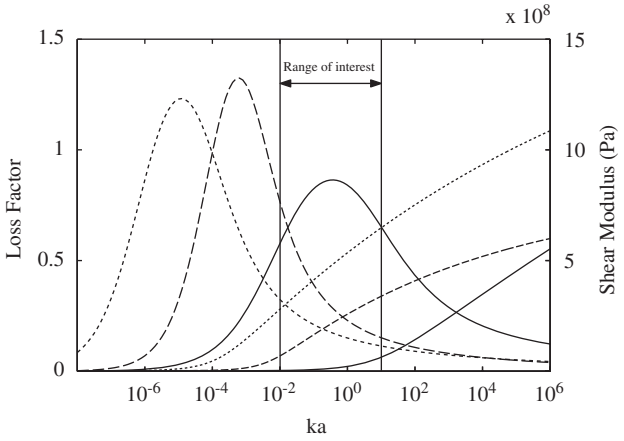

Fig. 2. The corresponding fit of HN equations for real part of the shear modulus and the loss factor for the selected polymers in a wide frequency range (—— η, polymer 2; – – – η, polymer 10; ····· η, polymer 16; ——, polymer 2; - - - - - G', polymer 10; ····· G', polymer 16).

where $\gamma = \alpha\pi/2$, and the loss factor is specified by

$$\eta(\omega) = \frac{G''(\omega)}{G'(\omega)} = \frac{(1-X)\sin(\beta\vartheta)}{[1+2\omega^{\alpha}\tau^{\alpha}\cos\gamma+\omega^{2\alpha}\tau^{2\alpha}]^{\beta/2}-(1-X)\cos(\beta\vartheta)} \tag{6}$$

in which

$$X = G_0/G_{\infty}, \quad \text{and} \quad \vartheta(\omega) = \tan^{-1}\frac{\omega^{\alpha}\tau^{\alpha}\sin\gamma}{1+\omega^{\alpha}\tau^{\alpha}\cos\gamma}.$$

Here we note that $\eta(\omega)$ depends only on the ratio $X = G_0/G_{\infty}$, not on their individual values. Furthermore, G_0 (relaxed modulus) and G_{∞} (unrelaxed modulus) are the limiting values of the shear modulus at low and high frequencies, respectively, $\tau(=1/\omega_0)$ is the relaxation time associated with the polymer glass transition centre frequency (loss factor peak), α is a dimensionless parameter ($0<\alpha<1$) that governs the width of the relaxation, and β is another dimensionless parameter ($0<\beta<1$) that governs the asymmetry of the relaxation.

The viscoelastic material under consideration is assumed to be linear, macroscopically homogeneous, and isotropic for which the constitutive equation, for harmonic time functions, may be written as [66]

$$\sigma_{ij} = \lambda^*(\omega)\delta_{ij}\varepsilon + 2\mu^*(\omega)\varepsilon_{ij}, \tag{7}$$

where δ_{ij} is Kronecker delta symbol, $\lambda^*(\omega)$ and $\mu^*(\omega)$ are complex, frequency-dependent Lame functions which are determined according to the standard relations

$$\lambda^*(\omega) = \frac{2v}{1-2v}G^*(\omega), \quad \mu^*(w) = G^*(w), \tag{8}$$

in which the real and imaginary parts of the complex shear modulus, $G^*(\omega)$, are specified in Eq. (5). Also, the wave motion inside the coating or core of the compound viscoelastic cylinder is governed by the classical Navier's equation [67]

$$\rho\frac{\partial^2\mathbf{u}}{\partial t^2} = \mu^*\nabla^2\mathbf{u} + (\lambda^*+\mu^*)\boldsymbol{\nabla}(\boldsymbol{\nabla}\cdot\mathbf{u}) \tag{9}$$

subject to the appropriate boundary conditions. Here, ρ is the solid material density, and $\mathbf{u}$ is the vector displacement that can advantageously be expressed as sum of the gradient of a scalar potential and the curl of a vector potential:

$$\mathbf{u} = \boldsymbol{\nabla}\phi + \boldsymbol{\nabla}\times\boldsymbol{\psi}, \tag{10}$$

with the condition $\boldsymbol{\nabla}\cdot\boldsymbol{\psi} = 0$, and noting the two-dimensional nature of the problem (i.e., the translational invariance of the incident sound field along the z-axis of the compound cylinder; see Fig. 1), we may adopt the simplifying assumption $\boldsymbol{\psi} = (0.,0.,\psi)$ [21]. The above decomposition enables us to separate the dynamic equation of motion into the classical Helmholtz equations:

$$\begin{aligned}(\nabla^2+k_c^2)\phi &= 0,\\ (\nabla^2+k_s^2)\psi &= 0,\end{aligned} \tag{11}$$

where k_c and k_s are complex wavenumbers, known as [66]

$$k_c = \frac{\omega}{\sqrt{(\lambda^*+2\mu^*)/\rho}}, \quad k_s = \frac{\omega}{\sqrt{\mu^*/\rho}}. \tag{12}$$

Furthermore, the relevant displacement components in polar coordinates in terms of compressional and shear wave potentials may simply written as [67]

$$\begin{aligned}u_r &= \frac{\partial\phi}{\partial r}+\frac{1}{r}\frac{\partial\psi}{\partial\theta},\\ u_\theta &= \frac{1}{r}\frac{\partial\phi}{\partial\theta}-\frac{\partial\psi}{\partial r}\end{aligned} \tag{13}$$

and the corresponding stresses in the viscoelastic compound cylinder are [67]

$$\sigma_{rr} = 2\mu^* \frac{\partial u_r}{\partial r} + \lambda^* \varepsilon,$$
$$\sigma_{r\theta} = \mu^* \left(\frac{1}{r} \frac{\partial u_r}{\partial \theta} + \frac{\partial u_\theta}{\partial r} - \frac{u_\theta}{r} \right), \tag{14}$$

where $\varepsilon = \nabla \cdot \mathbf{u} = \nabla^2 \phi = -k_c^2 \phi$.

The field expansions for the standing longitudinal and shear waves reverberating inside the coating material may be written as [21,29]

$$\phi_I = \sum_{n=-\infty}^{\infty} [B_n(\omega) J_n(k_c^I r_1) e^{in\theta_1} + C_n(\omega) H_n(k_c^I r_2) e^{in\theta_2}],$$
$$\psi_I = \sum_{n=-\infty}^{\infty} [D_n(\omega) J_n(k_s^I r_1) e^{in\theta_1} + E_n(\omega) H_n(k_s^I r_2) e^{in\theta_2}], \tag{15}$$

where B_n through E_n are unknown transmission coefficients and the index "I" throughout the formulation refers to the parameters associated with the coating material (Fig. 1). Moreover, the field expansions in the cylindrical core may be represented by [21]

$$\phi_{II}(r_2, \theta_2, \omega) = \sum_{n=-\infty}^{\infty} F_n(\omega) J_n(k_c^{II} r_2) e^{in\theta_2},$$
$$\psi_{II}(r_2, \theta_2, \omega) = \sum_{n=-\infty}^{\infty} G_n(\omega) J_n(k_s^{II} r_2) e^{in\theta_2}, \tag{16}$$

in which F_n and G_n are unknown coefficients and the index "II" throughout the formulation refers to the parameters associated with the core material (Fig. 1). The unknown coefficients $A_n(\omega)$ through $G_n(\omega)$ will be determined next by imposing the suitable boundary conditions.

2.3. Boundary conditions and addition theorem

The specific boundary conditions that have to be satisfied for the coating medium I in contact with the surrounding acoustic fluid (i.e., at $r_1 = a$) are [21]:

$$v_r = -i\omega u_r^I, \quad p = -\sigma_{rr}^I, \quad \sigma_{r\theta}^I = 0. \tag{17}$$

Also, at $r_2 = b$, the relevant displacement and stress components in the coating medium I must be equal to those in the core medium II [21]:

$$u_{r,\theta}^I = u_{r,\theta}^{II}, \quad \sigma_{rr,r\theta}^I = \sigma_{rr,r\theta}^{II}. \tag{18}$$

Now, to satisfy the above boundary conditions (fulfil orthogonality), a class of mathematical relationships called the addition theorems may advantageously be employed which in general allows one to translate the expressions of wave fields in different local coordinate systems into the same coordinate system (i.e., to study the fields scattered by the various interfaces, all referred to a common origin). Accordingly, we shall express the cylindrical wave functions of the first (second) coordinate system in terms of cylindrical wave functions of the second (first) coordinate system by application of the classical form of translational addition theorem for cylindrical Bessel functions [68]:

$$H_n(k_{c,s}^I r_2) e^{in\theta_2} = \sum_{m=-\infty}^{\infty} J_{m-n}(k_{c,s}^I d) H_m(k_{c,s}^I r_1) e^{im\theta_1},$$
$$J_n(k_{c,s}^I r_1) e^{in\theta_1} = \sum_{m=-\infty}^{\infty} J_{n-m}(k_{c,s}^I d) J_m(k_{c,s}^I r_2) e^{im\theta_2}. \tag{19}$$

The above addition theorem may advantageously be utilized in Eq. (15) to express the field potentials in the viscoelastic coating merely with respect to the first or the second coordinate system, i.e., we may either write

$$\phi_I(r_1,\theta_1,\omega)=\sum_{n=-\infty}^{\infty}[B_n(\omega)J_n(k_c^I r_1)\mathrm{e}^{\mathrm{i}n\theta_1}+\bar{C}_n(\omega)H_n(k_c^I r_1)\mathrm{e}^{\mathrm{i}n\theta_1}],$$
$$\psi_I(r_1,\theta_1,\omega)=\sum_{n=-\infty}^{\infty}[D_n(\omega)J_n(k_s^I r_1)\mathrm{e}^{\mathrm{i}n\theta_1}+\bar{E}_n(\omega)H_n(k_s^I r_1)\mathrm{e}^{\mathrm{i}n\theta_1}], \tag{20}$$

or

$$\phi_I(r_2,\theta_2,\omega)=\sum_{n=-\infty}^{\infty}[\bar{B}_n(\omega)J_n(k_c^I r_2)\mathrm{e}^{in\theta_2}+C_n(\omega)H_n(k_c^I r_2)\,\mathrm{e}^{in\theta_2}],$$
$$\psi_I(r_2,\theta_2,\omega)=\sum_{n=-\infty}^{\infty}[\bar{D}_n(\omega)J_n(k_s^I r_2)\mathrm{e}^{in\theta_2}+E_n(\omega)H_n(k_s^I r_2)\,\mathrm{e}^{in\theta_2}], \tag{21}$$

where

$$\bar{B}_n(\omega)=\sum_{m=-\infty}^{\infty}B_m(\omega)J_{m-n}(k_c^I d),\quad \bar{C}_n(\omega)=\sum_{m=-\infty}^{\infty}C_m(\omega)J_{n-m}(k_c^I d),$$
$$\bar{D}_n(\omega)=\sum_{m=-\infty}^{\infty}D_m(\omega)J_{m-n}(k_s^I d),\quad \bar{E}_n(\omega)=\sum_{m=-\infty}^{\infty}E_m(\omega)J_{n-m}(k_s^I d). \tag{22}$$

Finally, utilization of the expansions (2), (3), (16), (20) and (21) in the boundary conditions (17) and (18) yields

$$-kH_n'(k\mathrm{a})A_n+\mathrm{i}\omega k_c^I\mathrm{a}J_n'(k_c^I\mathrm{a})B_n+\mathrm{i}\omega k_c^I\mathrm{a}H_n'(k_c^I\mathrm{a})\bar{C}_n+\omega nJ_n(k_s^I\mathrm{a})D_n+\omega nH_n(k_s^I\mathrm{a})\bar{E}_n=\varphi_0\mathrm{i}^n k\mathrm{a}J_n'(k\mathrm{a})\mathrm{e}^{-\mathrm{i}n\alpha_0}, \tag{23a}$$

$$\mathrm{i}\omega\rho_0H_n(k\mathrm{a})A_n+[\lambda_I^*(k_c^I)^2J_n(k_c^I\mathrm{a})-2\mu_I^*(k_c^I)^2J_n''(k_c^I\mathrm{a})]B_n+[\lambda_I^*(k_c^I)^2H_n(k_c^I\mathrm{a})-2\mu_I^*(k_c^I)^2H_n''(k_c^I\mathrm{a})]\bar{C}_n-(2\mathrm{i}n\mu_I^*/\mathrm{a}^2)[J_n(k_s^I\mathrm{a})-\mathrm{a}k_s^IJ_n'(k_s^I\mathrm{a})]D_n-(2\mathrm{i}n\mu_I^*/\mathrm{a}^2)[H_n(k_s^I\mathrm{a})-\mathrm{a}k_s^IH_n'(k_s^I\mathrm{a})]\bar{E}_n=-\varphi_0\omega\rho_0\mathrm{i}^{n+1}\mathrm{e}^{-\mathrm{i}n\alpha_0}J_n(k\mathrm{a}), \tag{23b}$$

$$2\mathrm{i}n\mu_I^*[\mathrm{a}k_c^IJ_n'(k_c^I\mathrm{a})-J_n(k_c^I\mathrm{a})]B_n+2\mathrm{i}n\mu_I^*[\mathrm{a}k_c^IH_n'(k_c^I\mathrm{a})-H_n(k_c^I\mathrm{a})]\bar{C}_n-\mu_I^*[n^2J_n(k_s^I\mathrm{a})+\mathrm{a}^2(k_s^I)^2J_n''(k_s^I\mathrm{a})-\mathrm{a}k_s^IJ_n'(k_s^I\mathrm{a})]D_n-\mu_I^*[n^2H_n(k_s^I\mathrm{a})+\mathrm{a}^2(k_s^I)^2H_n''(k_s^I\mathrm{a})-\mathrm{a}k_s^IH_n'(k_s^I\mathrm{a})]\bar{E}_n=0, \tag{23c}$$

$$k_c^IbJ_n'(k_c^Ib)\bar{B}_n+k_c^IbH_n'(k_c^Ib)C_n+\mathrm{i}nJ_n(k_s^Ib)\bar{D}_n+\mathrm{i}nH_n(k_s^Ib)E_n-k_c^{II}bJ_n'(k_c^{II}b)F_n-\mathrm{i}nJ_n(k_s^{II}b)G_n=0, \tag{23d}$$

$$\mathrm{i}nJ_n(k_c^Ib)\bar{B}_n+\mathrm{i}nH_n(k_c^Ib)C_n-k_s^IbJ_n'(k_s^Ib)\bar{D}_n-k_s^IbH_n'(k_s^Ib)E_n-\mathrm{i}nJ_n(k_c^{II}b)F_n+k_s^{II}bJ_n'(k_s^{II}b)G_n=0, \tag{23e}$$

$$[\lambda_I^*(k_c^I)^2J_n(k_c^Ib)-2\mu_I^*(k_c^I)^2J_n''(k_c^Ib)]\bar{B}_n+[\lambda_I^*(k_c^I)^2H_n(k_c^Ib)-2\mu_I^*(k_c^I)^2H_n''(k_c^Ib)]C_n-(2\mathrm{i}n\mu_I^*/b^2)[J_n(k_s^Ib)-bk_s^IJ_n'(k_s^Ib)]\bar{D}_n-(2\mathrm{i}n\mu_I^*/b^2)[H_n(k_s^Ib)-bk_s^IH_n'(k_s^Ib)]E_n-[\lambda_{II}^*(k_c^{II})^2J_n(k_c^Ib)-2\mu_{II}^*(k_c^{II})^2J_n''(k_c^Ib)]F_n+(2\mathrm{i}n\mu_{II}^*/b^2)[J_n(k_s^{II}b)-bk_s^{II}J_n'(k_s^{II}b)]G_n=0, \tag{23f}$$

$$
\begin{aligned}
&2in\mu_I^*[bk_c^I J_n'(k_c^I b) - J_n(k_c^I b)]\bar{B}_n + 2in\mu_I^*[bk_c^I H_n'(k_c^I b) - H_n(k_c^I b)]C_n \\
&\quad - \mu_I^*[n^2 J_n(k_s^I b) + b^2(k_s^I)^2 J_n''(k_s^I b) - bk_s^I J_n'(k_s^I b)]\bar{D}_n \\
&\quad - \mu_I^*[n^2 H_n(k_s^I b) + b^2(k_s^I)^2 H_n''(k_s^I b) - bk_s^I H_n'(k_s^I b)]E_n \\
&\quad - 2in\mu_{II}^*[bk_c^{II} J_n'(k_c^{II} b) - J_n(k_c^{II} b)]F_n + \mu_{II}^*[n^2 J_n(k_s^{II} b) \\
&\quad + b^2(k_s^{II})^2 J_n''(k_s^{II} b) - bk_s^{II} J_n'(k_s^{II} b)]G_n = 0.
\end{aligned} \tag{23g}
$$

This completes the necessary background required for the exact analysis of the problem. Next we consider some numerical examples.

3. Numerical results

In order to illustrate the nature and general behaviour of solution, we consider a number of specific numerical examples in this section. Realizing the large number of parameters involved here, no attempt is made to exhaustively evaluate the effect of varying each of them. Thus, our attention is confined to a particular model. The ambient fluid is assumed to be water at atmospheric pressure and room temperature ($\rho_0 = 1000\,\mathrm{kg/m^3}$, $c_0 = 1485\,\mathrm{m/s}$). Two general combinations of constituent materials for the core and coating are considered. In the first case, the inner core of the compound cylinder is supposed to be fabricated from steel ($\rho_{II} = 7850\,\mathrm{kg/m^3}$, $\lambda_{II}^* = 121.15 \times 10^9$, $\mu_{II}^* = 80.77 \times 10^9$) while the outer coating is elastomeric with a fixed radius of $b = 1\,\mathrm{cm}$ for selected thickness ratio parameters ($b/\mathrm{a} = 0.5, 0.75, 0.9$). In the second case, the situation is reversed, i.e., the eccentric shell is made of steel and is filled with polymeric materials. Hartmann et al. [42], for the first time, reported all the input parameters necessary for a complete description of viscoelastic material properties for a set of polyurethane polymers within the context of Havriliak–Negami theory. The HN fitting parameters for three selected polymers with distinctively different dynamic viscoelastic properties (i.e., polymers 2, 10 and 16) in the frequency range of our interest are compiled in Table 1. The corresponding fit of HN equations for shear moduli, (ω), and loss factor, $\eta(\omega)$, (i.e., the first of Eqs. (5) and (6)) for the selected polymers in a relatively wide frequency range, are displayed in Fig. 2. Polymer 2 is found to basically have the highest damping (loss factor), and polymer 16 is found to have the lowest damping in the frequency range of our interest.

Accurate computation of cylindrical Bessel functions is achieved by employing the relevant MATLAB specialized math functions. Computations for derivatives of cylindrical Bessel functions were accomplished by utilizing (9.1.27) in the handbook by Abramowitz and Stegun [61]. A MATLAB code was constructed for treating boundary conditions, to determine the unknown scattering/transmission coefficients, and other relevant acoustic field quantities as a function of non-dimensional frequency, $ka = \omega a/c_0$, at selected core eccentricity parameters, $e = d/(a-b)$. The computations were performed on a Pentium IV personal computer with a maximum truncation constant of $n_{\max} = m_{\max} = 30$ to assure convergence in the high-frequency range, and also in case of high core eccentricity. The convergence of numerical solutions were systematically checked in a simple trial and error manner, by increasing the truncation constants (i.e., including higher number of modes) while looking for steadiness or stability in the numerical value of the solutions [38].

Table 1
Havriliak–Negami fitting parameters

Parameter	Polymer 2	Polymer 10	Polymer 16
G_0 (MPa)	1.558	2.243	1.728
G_∞ (GPa)	3.573	0.8208	1.888
τ (s)	1.574×10^{-6}	3.107×10^{-3}	8.268×10^{-2}
α	0.5332	0.7236	0.6602
β	0.0269	0.0935	0.0574
ρ (kg/m^3)	1092	1106	1170
ν	0.4	0.4	0.4

The most relevant acoustic field quantity is the (far-field) scattering form function amplitude, with the standard definition [69]:

$$|f_\infty(r_1,\theta_1=\pi+\alpha_0,\omega)| \approx \lim_{r_1\to\infty}\left|\sqrt{\frac{2r_1}{\mathrm{a}}}\frac{\varphi_{\mathrm{scat.}}(r_1,\theta_1,\omega)}{\varphi_{\mathrm{inc.}}}\right| \tag{24}$$

The two most important incidence angles are $\alpha_0=0$ (end-on) and $\alpha_0=\pi/2$ (broadside), as they best help to expose the physics of the problem. Figs. 3–5 displays the variation of the backscattered form function amplitude with ka for end-on ($\alpha_0=0$) and broadside ($\alpha_0=\pi/2$) incidence upon a compound cylinder with viscoelastic coating and steel core for selected core eccentricities ($e=0\%$, 25%, 50%, 75%, 90%), coating thicknesses ($b/\mathrm{a}=0.5$,0.75,0.9) and material types (i.e., polymers 2,10,16). Careful examination of the figure leads to the following important observations. The form function curves associated with polymer 2 (polymers 10 and 16), which is highly (are lightly) damped at intermediate and high dimensionless frequencies (see Fig. 2), exhibits a distinctively inferior oscillatory (show a highly resonatory) behaviour at these frequencies, especially in the end-on incidence ($\alpha_0=0$) situation. At very low wavenumbers, there is a single notable sharp resonance in the response spectra (i.e., at $k\mathrm{a}\approx 0.18$) for the polymer 2 coating, which is clearly linked to its relatively low level of damping at these frequencies. The response spectra for polymers 10 and 16, on the other hand, show no sign of a resonance excitation, which is undoubtedly related to their relatively high level of damping at very low frequencies (see Fig. 2). Core eccentricity has a notable effect on the form function spectra for the compound cylinder with a relatively thick coating ($b/\mathrm{a}=0.5$), especially for polymer 10 (polymer 2) in the end-on (broadside) incidence case. Decreasing coating thickness leads to a natural decrease in the effect of core eccentricity, while numerous sharp peaks in the resonance spectrum begin to appear in the intermediate and high-frequency range. The latter effect may clearly be linked to the revealing of resonances associated with the steel core. This effect can even be observed in case of polymer 2 coating, which has the highest damping in the intermediate and high-frequency range (e.g., note several relatively large amplitude peaks appearing in the associated form function spectrum in Fig. 5).

Increasing core eccentricity in the end-on incidence case leads to an interesting behaviour in the backscattered spectrum, especially for the compound cylinder with a thick coating ($b/\mathrm{a}=0.5$). In particular, Fig. 3 shows that increasing core eccentricity in the end-on incidence situation causes overall dampening of resonances for the compound cylinder with polymer 10 (polymer 16) coating in the low (low and intermediate) frequency range. This may be linked to the fact that the incident wave encounters increasingly more dissipative material with increasing core eccentricity for this angle of incidence. Another interesting effect of increasing core eccentricity is appearance of a whole new set of resonance frequencies which seem to be absent in case of a compound cylinder with a concentric core (i.e., some of the modes which cannot be regularly excited in the concentric case, will be excited as the compound cylinder becomes eccentric). This can even be clearly observed for example in the form function spectrum associated with the highly damped polymeric coating no. 2, which exhibits several (single or compound) large peaks as the core becomes non-concentric in the broadside incidence situation (see Figs. 3 and 4). Furthermore, in the eccentric situation, some of the resonances shift to the lower frequencies, while they may also bifurcate (e.g., note the compound resonances observed for polymer 2 coating for some eccentricities in the second columns of Figs. 4 and 5). The latter observation is also in accordance with the findings of Danila et al. [70], who noted a decrease in some of the resonance frequencies in addition to observation of the bifurcation effect for a metallic shell of non-uniform wall thickness as the core eccentricity increases (see their Figs. 2 and 6).

Figs. 6–8 displays the variation of the backscattered form function amplitude with ka for broadside/end-on incidence upon a compound cylinder with steel casing and viscoelastic core for selected core material types, shell thicknesses and core eccentricities. Comments as in above discussions may readily be made. The most important distinctions are as follows. When the shell thickness is comparable to core size ($b/\mathrm{a}=0.5$), the type of viscoelastic core material has nearly no effect on the backscattered form function amplitude, irrespective of core eccentricity and/or angle of incidence (Fig. 6). This is clearly due to relatively high impedance of the massive shell in comparison with the viscoelastic filling material. As the shell thickness decreases ($b/\mathrm{a}=0.75$,0.9), the effect of dynamic viscoelastic properties of the core gradually becomes more evident. Nevertheless, even in case of a relatively thin coating (i.e., a comparatively thick viscoelastic core, $b/\mathrm{a}=0.9$),

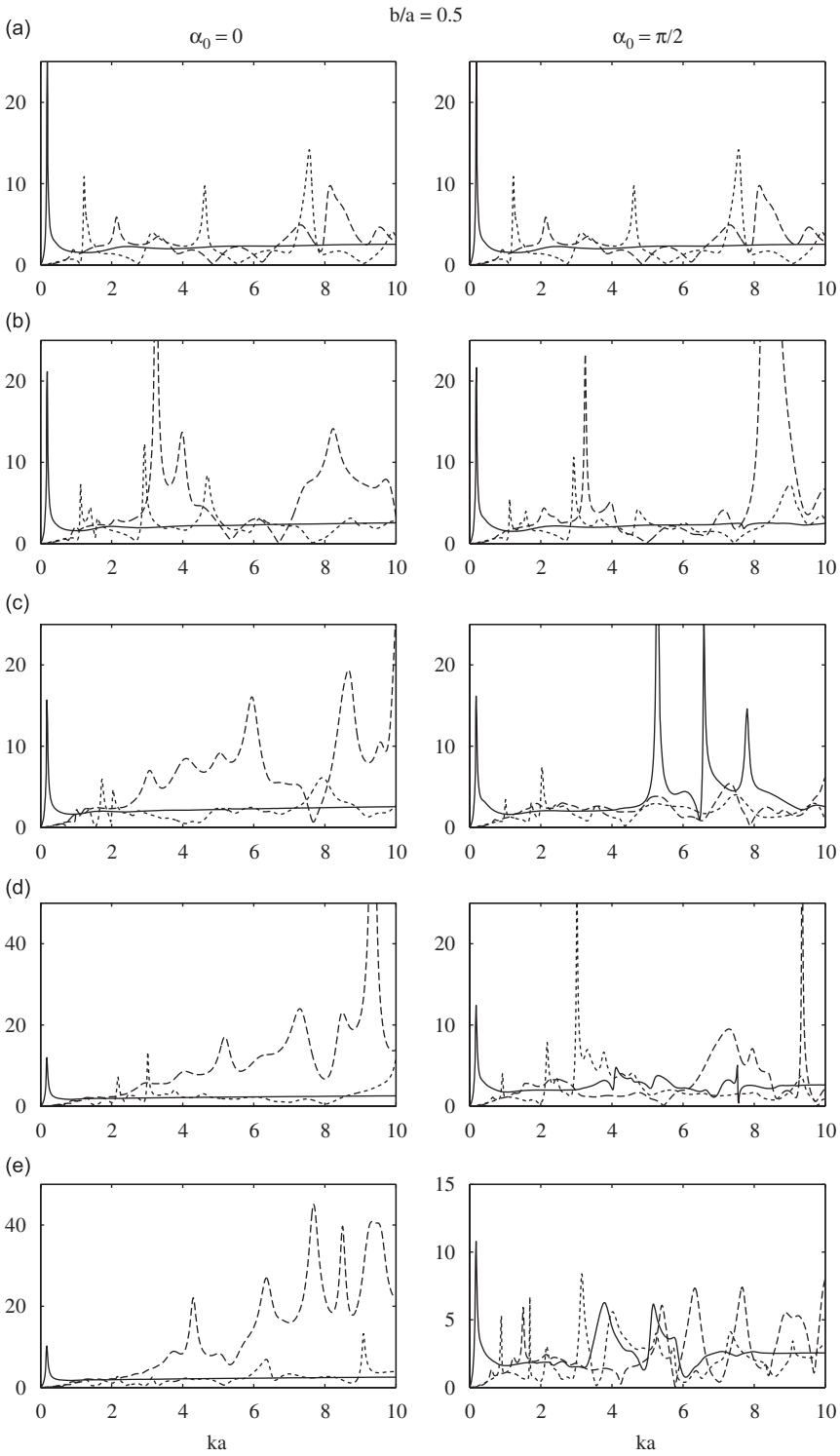

Fig. 3. Variation of the backscattered form function amplitude with dimensionless frequency for broadside and end-on incidence upon a compound cylinder with viscoelastic coating and steel core for selected core eccentricities, coating thickness (b/a = 0.5) and material types; (a) $e = 0\%$, (b) $e = 25\%$, (c) $e = 50\%$, (d) $e = 75\%$, (e) $e = 90\%$, (—— polymer 2; – – – – polymer 10; ⋯⋯ polymer 16).

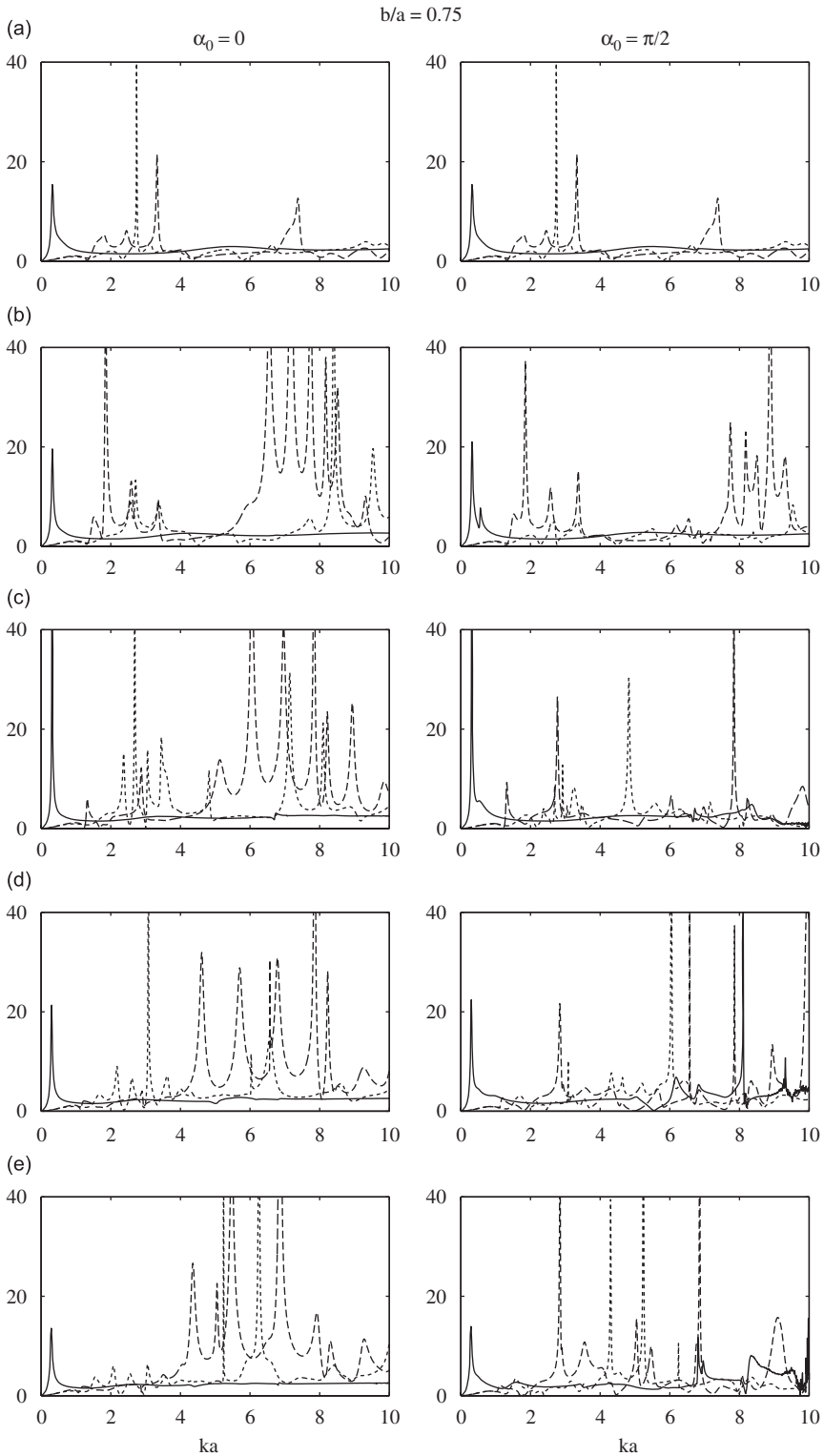

Fig. 4. Variation of the backscattered form function amplitude with dimensionless frequency for broadside and end-on incidence upon a compound cylinder with viscoelastic coating and steel core for selected core eccentricities, coating thickness (b/a = 0.75) and material types; (a) $e = 0\%$, (b) $e = 25\%$, (c) $e = 50\%$, (d) $e = 75\%$, (e) $e = 90\%$, (—— polymer 2; −−−− polymer 10; ····· polymer 16).

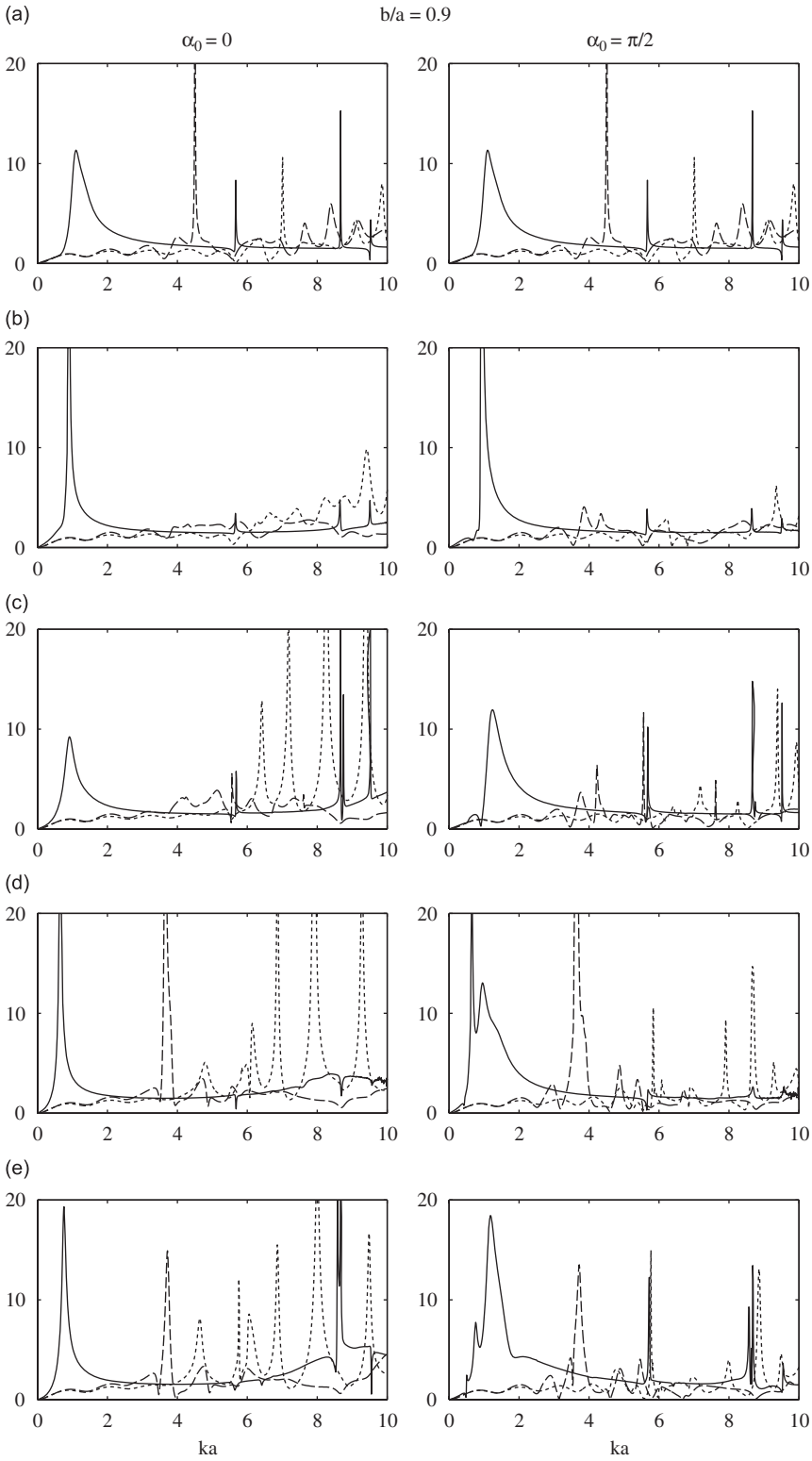

Fig. 5. Variation of the backscattered form function amplitude with dimensionless frequency for broadside and end-on incidence upon a compound cylinder with viscoelastic coating and steel core for selected core eccentricities, coating thickness ($b/a = 0.9$) and material types; (a) $e = 0\%$, (b) $e = 25\%$, (c) $e = 50\%$, (d) $e = 75\%$, (e) $e = 90\%$, (—— polymer 2; – – – – polymer 10; ⋯⋯ polymer 16).

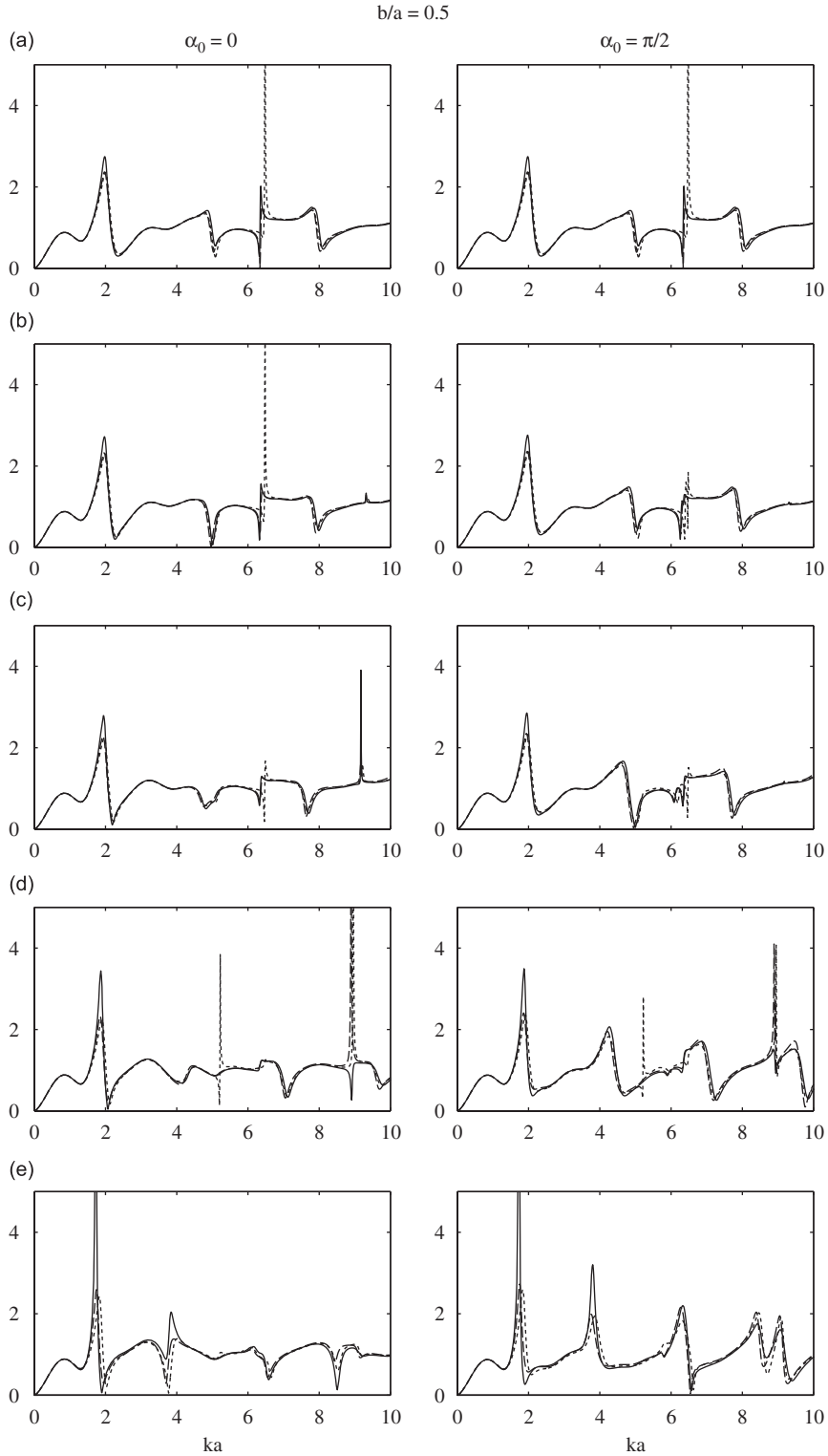

Fig. 6. Variation of the backscattered form function amplitude with dimensionless frequency for broadside/end-on incidence upon a compound cylinder with steel casing and viscoelastic core for selected core material types, shell thickness ($b/a = 0.5$) and core eccentricities; (a) $e = 0\%$, (b) $e = 25\%$, (c) $e = 50\%$, (d) $e = 75\%$, (e) $e = 90\%$, (—— polymer 2; – – – – polymer 10; ⋯⋯ polymer 16).

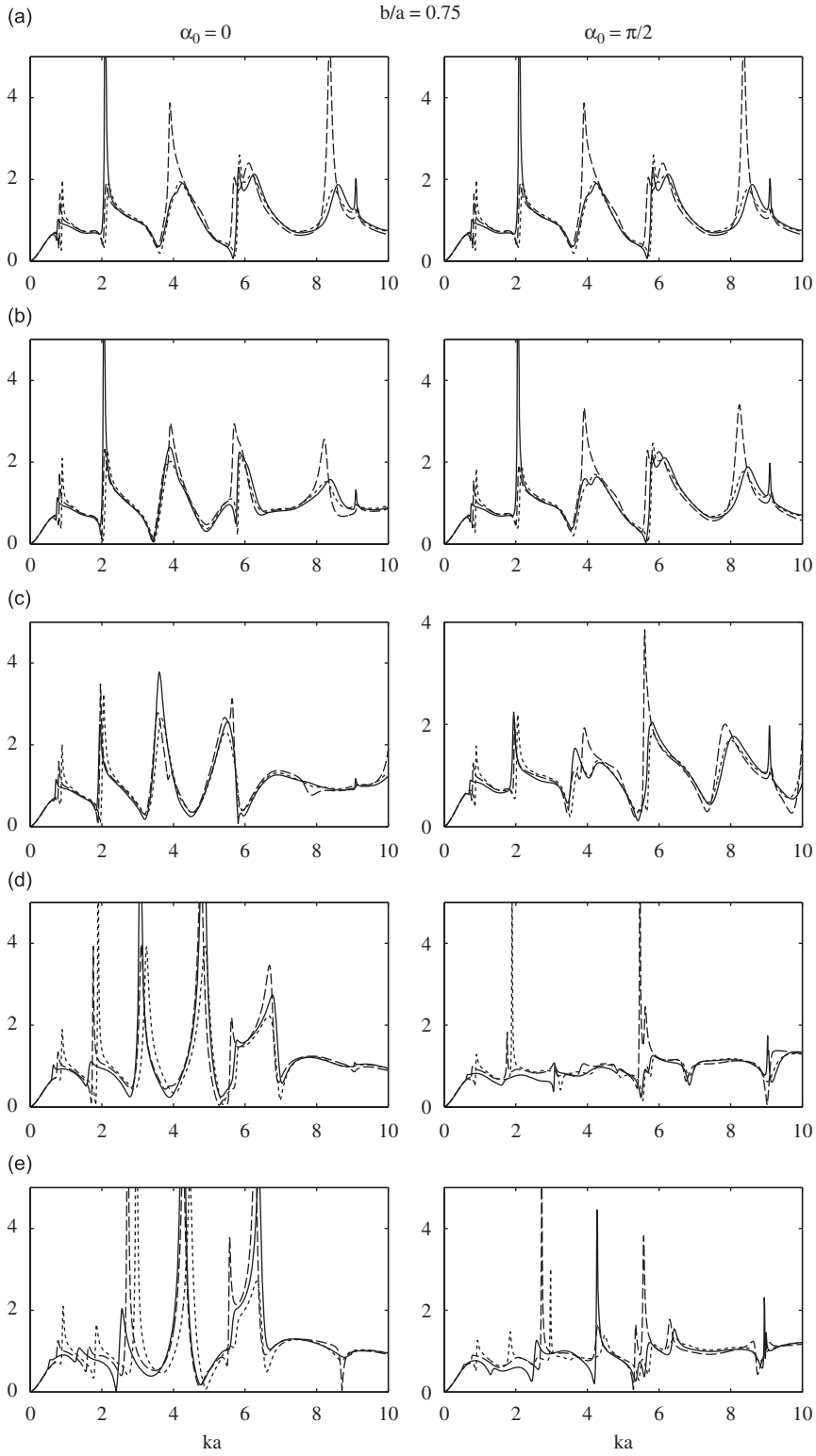

Fig. 7. Variation of the backscattered form function amplitude with dimensionless frequency for broadside/end-on incidence upon a compound cylinder with steel casing and viscoelastic core for selected core material types, shell thickness ($b/a = 0.75$) and core eccentricities; (a) $e = 0\%$, (b) $e = 25\%$, (c) $e = 50\%$, (d) $e = 75\%$, (e) $e = 90\%$, (—— polymer 2; – – – – polymer 10; ⋯⋯ polymer 16).

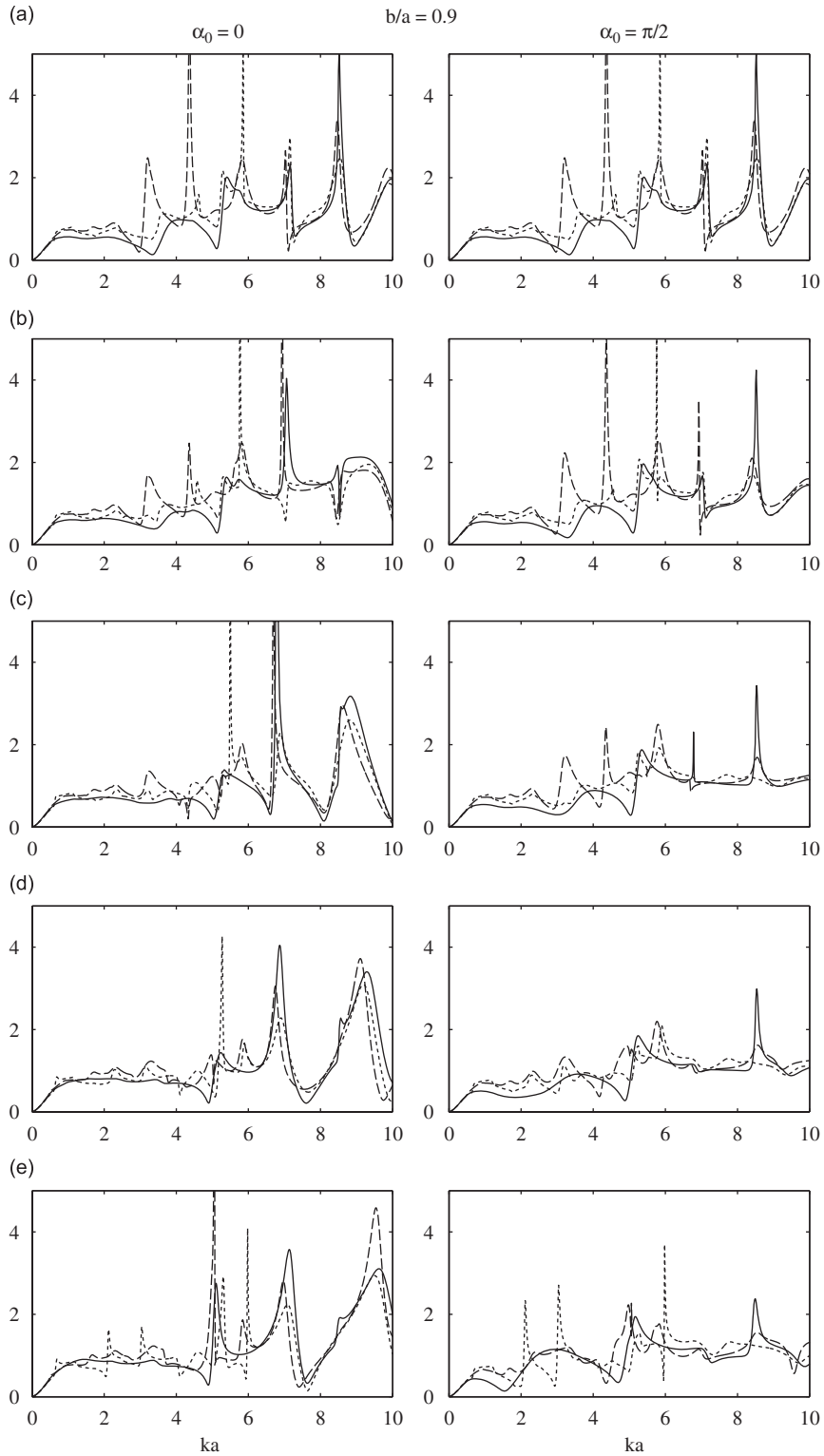

Fig. 8. Variation of the backscattered form function amplitude with dimensionless frequency for broadside/end-on incidence upon a compound cylinder with steel casing and viscoelastic core for selected core material types, shell thickness ($b/a = 0.9$) and core eccentricities; (a) $e = 0\%$, (b) $e = 25\%$, (c) $e = 50\%$, (d) $e = 75\%$, (e) $e = 90\%$, (—— polymer 2; – – – – polymer 10; ⋯⋯ polymer 16).

the effect of changing polymer type is not perhaps as great as it was originally expected, nearly irrespective of core eccentricity or angle of incidence (e.g., in comparison with the relatively remarkable effects observed in Figs. 3–5 for the viscoelastically coated cylinders). Furthermore, as the viscoelastic core eccentricity increases, most of the resonances shift to the lower frequencies, while very few of them may bifurcate (i.e., in comparison with the notable number of compound resonances observed for some eccentricities in Figs. 4 and 5). This notable leftward shift of resonances may be explained by the fact that as the viscoelastic core eccentricity increases (steel shell thickness in some parts decreases), the overall stiffness of the compound cylinder in the

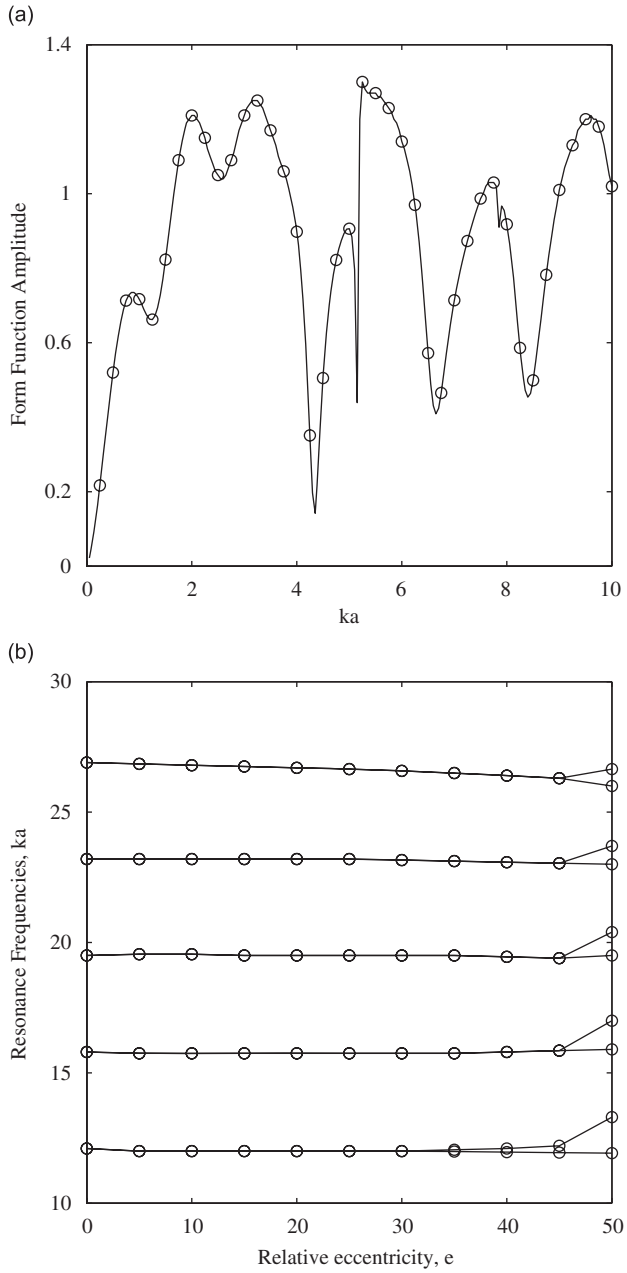

Fig. 9. (a) Backscattered form function amplitude versus nondimensional frequency for normal incidence upon a copper-clad concentric aluminium rod immersed in water (—— Honarvar and Sinclair's results [16]; ○ present results). (b) The first few modal resonance frequencies versus relative eccentricity for a water submerged and air-filled eccentric aluminium shell (—— Danila et al.'s results [70]; ○ present results).

region in which the surface waves predominantly propagate effectively decreases. The latter observation is especially true for polymer 2 (i.e., the polymer with the lowest shear moduli G'; see Fig. 2) for which the highest amount of leftward shift in the resonances are observed (e.g., see Fig. 7). As the stiffness of viscoelastic core increases, this leftward shift decreases (e.g., see Fig. 7 where polymer 16 which has the highest stiffness shows the smallest amount of shift).

Finally, in order to check overall validity of the calculations, we first computed the backscattered form function amplitude, $|f_\infty(r_1,\theta_1=\pi,\omega)|$, versus non-dimensional frequency for normal incidence upon a copper-clad concentric aluminium rod immersed in water by setting, $d=0$, a $=0.915$ cm, $b=0.870$ cm, $\rho_I=8900$, $\rho_{II}=2694$, $\mu_I^*=5.39\times10^{10}$, $\mu_{II}^*=2.6\times10^{10}$, $\lambda_I^*=8.06\times10^{10}$, and $\lambda_{II}^*=5.91\times10^{10}$ in our general MATLAB code. Fig. 9a demonstrates that our numerical results closely follow the numerical data extracted from Fig. 2 in Ref. [16]. As a further check, we computed the first few modal resonance frequencies [71] versus relative eccentricity for a water submerged and air-filled eccentric aluminium shell. The outcome as displayed in Fig. 9b shows good agreement with the numerical results presented in Fig. 2 of Ref. [70].

4. Conclusions

Various complicating effects such as material viscoelasticity and/or core eccentricity can exist in compound cylindrical components that can obscure the acoustic analysis of such structures. This work presents analytical solutions as well as numerical results for two-dimensional scattering of plane sound waves by an eccentric compound circular cylinder including dynamic viscoelastic effects. The solution is based on the translational addition theorem for cylindrical wave functions and the Havriliak–Negami viscoelastic model which is among the most successful descriptions for the frequency dependence of the complex modulus of polymeric materials in the glass transition region. The far-field backscattered form function amplitude spectra is computed for selected materials, angles of incidence, incident wave frequencies, core eccentricities, and coating thicknesses. The most important observations for a metallic cylinder (steel rod) eccentrically coated with viscoelastic materials are as follows. At very low dimensionless frequencies, the response spectra for polymers 10 and 16 (polymer 2) display no sign of a resonance excitation (displays a single notable sharp peak), which is linked to their (its) relatively high (low) level of damping at these frequencies. The form function curves associated with polymer 2 (polymers 10 and 16), which is highly (are lightly) damped at intermediate and high frequencies, exhibits a distinctively inferior oscillatory (show a highly resonatory) behaviour at these frequencies, especially in the end-on incidence situation. Decreasing the viscoelastic coating thickness leads to a natural decrease in the effect of core eccentricity, while numerous large amplitude sharp peaks in the resonance spectrum appear in the intermediate and high-frequency range which is primarily linked to the revealing of resonances associated with the metallic core, especially for the low damping polymers 10 and 16. For the compound cylinder with a thick polymer 10 (polymer 16) coating, increasing core eccentricity in the end-on incidence case causes overall dampening of resonances in the low (low and intermediate) frequency range. This is explained by the fact that the incident wave encounters increasingly more dissipative material with increasing core eccentricity for this angle of incidence. Furthermore, increasing core eccentricity leads to appearance of a whole new set of resonance frequencies which seem to be absent in case of a compound cylinder with a concentric metallic core (i.e., some of the modes which cannot be regularly excited in the concentric case, are excited as the compound cylinder becomes eccentric). Moreover, some of the resonances shift to the lower frequencies, while they may also bifurcate (i.e., some of the resonances become compound) in the eccentric core situation.

The key observations for an eccentric metallic (steel) shell filled with viscoelastic materials are as follows. When the shell thickness is comparable to the elastomeric core size, the type of viscoelastic material has nearly no effect on the backscattered spectra, irrespective of core eccentricity and/or angle of incidence. As the shell thickness decreases, the effect of dynamic viscoelastic material properties of the core gradually becomes more pronounced. Furthermore, as the viscoelastic core eccentricity increases, many of the resonances shift leftward to the lower frequencies, while few of them may bifurcate. This may be explained by the fact that as the metallic shell thickness in some parts decreases, the overall stiffness of the compound cylinder in the region in which the surface waves predominantly propagate effectively declines. Moreover, as the stiffness of viscoelastic core increases (e.g., for polymer 16), the above noted leftward shift decreases. The proposed model

demonstrates the call for consideration of core eccentricity (coating non-uniformity) in addition to the dynamic viscoelastic material properties in acoustic analysis (non-destructive characterization) of cladded cylindrical components.

References

[1] M.C. Junger, J.M. Garrelick, Short-wavelength backscattering cross section of rigid and partially coated cylinders and spheres, *Journal of the Acoustical Society of America* 56 (1974) 1347–1353.

[2] G.C. Gaunaurd, Sonar cross section of a coated hollow cylinder in water, *Journal of the Acoustical Society of America* 61 (1977) 360–368.

[3] G.C. Gaunaurd, High-frequency acoustic scattering from submerged cylindrical shells coated with viscoelastic absorbing layers, *Journal of the Acoustical Society of America* 62 (1977) 503–512.

[4] R.D. Doolittle, H. Uberall, Sound scattering by elastic cylindrical shells, *Journal of the Acoustical Society of America* 39 (1966) 272–275.

[5] W.G. Neubauer, Procedure for evaluating a reflection-reduction coating, *Journal of the Acoustical Society of America* 62 (1977) 1024–1027.

[6] L. Flax, W.G. Neubauer, Acoustic reflection from layered elastic absorptive cylinders, *Journal of the Acoustical Society of America* 61 (1977) 307–312.

[7] V.B. Poruchikov, A.V. Stepanov, Diffraction of an acoustic wave by a cylinder covered by a layer of soft material, *Fluid Mechanics, Soviet Research* 16 (l) (1987) 63–70.

[8] V.M. Ayres, G.C. Gaunaurd, Acoustic resonance scattering by viscoelastic objects, *Journal of the Acoustical Society of America* 81 (1987) 301–311.

[9] J. Sinai, R.C. Waag, Ultrasonic scattering by two concentric cylinders, *Journal of the Acoustical Society of America* 83 (1988) 1728–1735.

[10] K.S. Adamova, M.A. Kanibolotskii, Optimizing the structure of a cylindrically laminar coating for interaction with a plane acoustic wave, *Mechanics of Composite Materials* 26 (4) (1991) 468–473.

[11] A.A. Ferri, J.H. Ginsberg, P.H. Roger, Scattering of plane waves from submerged objects with partially coated surfaces, *Journal of the Acoustical Society of America* 92 (1992) 1721–1728.

[12] A.N. Sinclair, R.C. Addison, Acoustic diffraction spectrum of a SiC fiber in a solid elastic medium, *Journal of the Acoustical Society of America* 94 (1993) 126–135.

[13] B. Laulagnet, J.L. Guyader, Sound radiation from finite cylindrical coated shells, by means of asymptotic expansion of three-dimensional equations for coating, *Journal of the Acoustical Society of America* 96 (1994) 277–286.

[14] B. Laulagnet, J.L. Guyader, Sound radiation from finite cylindrical shells, partially covered with longitudinal strips of compliant layer, *Journal of sound and vibration* 186 (1995) 723–742.

[15] C. Partridge, Acoustic scattering from viscoelastically coated bodies, *Journal of the Acoustical society of America* 99 (1996) 72–78.

[16] F. Honarvar, A.N. Sinclair, Scattering of an obliquely incident plane wave from a circular clad rod, *Journal of the Acoustical society of America* 102 (1997) 41–48.

[17] J.H. Ginsberg, On the effect of viscosity in scattering from partially coated infinite cylinders, *Journal of the Acoustical Society of America* 112 (1) (2002) 46–54.

[18] J.M. Cuschieri, D. Feit, Influence of circumferential partial coating on the acoustic radiation from a fluid-loaded shell, *Journal of the Acoustical society of America* 107 (2000) 3196–3207.

[19] D. Luo, M. Cai, X. Peng, B. Luo, Analysis of sound radiation from the ring-stiffened cylindrical shell coated with viscoelastic layer in fluid medium, *Acta Mechanica Solida Sinica* 16 (2) (2003) 155–161.

[20] Y. Fan, B. Tysoe, J. Sim, K. Mirkhani, A.N. Sinclair, F. Honarvar, H. Sildva, A. Szecket, R. Hardwick, Nondestructive evaluation of explosively welded clad rods by resonance acoustic spectroscopy, *Ultrasonic* 41 (2003) 369–375.

[21] S.M. Hasheminejad, N. Safari, Acoustic scattering from viscoelastically coated spheres and cylinders in viscous fluids, *Journal of Sound and Vibration* 280 (2005) 101–125.

[22] V.P. Ivanov, Analysis of the field diffracted by a cylinder with a perforated coating, *Acta Acustica* 28 (6) (2003) 486–493.

[23] F.G. Mitri, Acoustic radiation force due to incident plane-progressive waves on coated cylindrical shells immersed in ideal compressible fluids, *Wave Motion* 43 (2006) 445–457.

[24] J.M. Cuschieri, The modeling of the radiation and response Green's function of a fluid-loaded cylindrical shell with an external compliant layer, *Journal of the Acoustical society of America* 119 (2006) 2150–2169.

[25] J.N. Barshinger, J.L. Rose, Guided wave propagation in an elastic hollow cylinder coated with a viscoelastic material, *IEEE Transactions on Ultrasonics, Ferroelectrics, and Frequency Control* 51 (11) (2004) 1547–1556.

[26] J.A. Roumeliotis, J.G. Fikioris, G.P. Gounaris, Electromagnetic scattering from an eccentrically coated infinite metallic cylinder, *Journal of Applied Physics* 51 (8) (1980) 4488–4493.

[27] Z.X. Shen, Electromagnetic scattering by an impedance cylinder coated eccentrically with a chiroplasma cylinder, *IEE Proceedings: Microwaves, Antennas and Propagation* 141 (4) (1994) 279–284.

[28] S.F. Morse, Z.W. Feng, P.L. Marston, High-frequency threshold processes for leaky waves on cylinders of variable thickness: fluid shell case, *Journal of the Acoustical society of America* 98 (1995) 2928.

[29] J.A. Roumeliotis, B. Kakogiannos, Acoustic scattering from an infinite cylinder of small radius coated by a penetrable one, *Journal of the Acoustical society of America* 97 (1995) 2074–2081.
[30] E.B. Danila, J.M. Conoir, J.L. Izbicki, Generalized Debye series expansion: treatment of the concentric and nonconcentric cylindrical fluid–fluid interfaces, *Journal of the Acoustical society of America* 98 (1995) 3326.
[31] E.B. Danila, J.M. Conoir, J.L. Izbicki, Generalized Debye series expansion. Part II, treatment of eccentric fluid–solid cylindrical interfaces, *Acta Acustica* 84 (1998) 38–44.
[32] J.A. Roumeliotis, S.P. Savaidis, Scattering by an infinite circular dielectric cylinder coating eccentrically an elliptic metallic one, *Transactions on Antennas and Propagation* 44 (5) (1996) 757–763.
[33] W.Y. Yin, H.L. Zhao, W. Wan, Parametric study on the scattering characteristics of two impedance cylinders eccentrically coated with Faraday chiral materials, *Electromagnetic Waves and Applications* 10 (11) (1996) 1467–1484.
[34] S.G. Tanyer, R.G. Olsen, High-frequency scattering by a conducting circular cylinder coated with a lossy dielectric of nonuniform thickness, *IEEE Transactions on Antennas and Propagation* 45 (4) (1997) 689–697.
[35] S.P. Savaidis, J.A. Roumeliotis, Scattering by an infinite elliptic dielectric cylinder coating eccentrically a circular metallic or dielectric cylinder, *IEEE Transactions on Microwave Theory and Techniques* 45 (10) (1997) 1792–1800.
[36] H.A. Yousif, A.Z. Elsherbeni, Oblique incidence scattering from two eccentric cylinders, *Journal of Electromagnetic Waves and Applications* 11 (9) (1997) 1273–1288.
[37] A.G. Simao, L.G. Guimaraes, J.P.R.F. de Mendonca, Electromagnetic stress on resonant light scattering by a cylinder with an eccentric inclusion, *Optics Communications* 170 (1999) 137–148.
[38] S.M. Hasheminejad, M. Azarpeyvand, Energy distribution and radiation loading of a cylindrical source suspended within a nonconcentric fluid cylinder, *Acta Mechanica* 164 (2003) 15–30.
[39] S.P. Savaidis, J.A. Roumeliotis, Scattering by an infinite circular dielectric cylinder coating eccentrically an elliptic dielectric cylinder, *IEEE Transactions on Antennas and Propagation* 52 (5) (2004) 1180–1185.
[40] B. Hu, Y.K. Edward, J. Zhang, S. Toutain, Scattering characteristics of conducting cylinder coated with nonuniform magnetized ferrite, *Chinese Physics* 14 (11) (2005) 2305–2313.
[41] M.A. Mushref, Closed solution to electromagnetic scattering of a plane wave by an eccentric cylinder coated with metamaterials, *Optics Communications* 270 (2007) 441–446.
[42] B. Hartman, G.F. Lee, J.D. Lee, Loss factor height and width limits for polymer relaxations, *Journal of the Acoustical society of America* 95 (1) (1994) 226–233.
[43] W.M. Davis, J.P. Szabo, Group contribution analysis applied to the Havriliak–Negami model for polyurethanes, *Computational and Theoretical Polymer Science* 11 (2001) 9–15.
[44] T.N. Baranova, Yu.F. Romanenko, B.P. Titkov, L.G. Chibirova, Device for checking the eccentricity of welding electrode coatings, *Soviet Energy Technology* 7 (1987) 77–79.
[45] E. Frevert, Continuous measurement of the sheating of insulated wire, *Wire World International* 29 (3) (1987) 69–70.
[46] A. Hadjoudj, J.C. David, J. Bouzon, J.M. Vergnaud, Modelling of heat treatment of a silicone rubber coating of an electrical wire, and applications to the mechanical properties, *Journal of Polymer Engineering* 8 (1-2) (1988) 93–109.
[47] G.R. Symmons, A.H. Menon, Z. Ming, M.S.J. Hashmi, Polymer coating of wire using a die-less drawing process, *Journal of Materials Processing Technology* 26 (2) (1991) 173–180.
[48] F. Honarvar, A.N. Sinclair, Nondestructive evaluation of cylindrical components by resonance acoustic spectroscopy, *Ultrasonics* 36 (1998) 845–854.
[49] J.W. Pilarczyk, Z. Muskalski, H. Dyja, B. Golis, Coating steel wires by polymers in hydrodynamic drawing, *Wire Journal International* 35 (8) (2002) 93–98.
[50] R.F. Anastasi, E.I. Madaras, Investigating the use of ultrasonic guided waves for aging wire insulation assessment, *Proceedings of SPIE—The International Society for Optical Engineering* 4702 (2002) 76–82.
[51] O.C. Davidson, S.C. Browning, An axially compressed, cylindrical shell with a viscoelastic core, *AIAA Journal* 2 (11) (1964) 2015.
[52] A.E. Bogdanovich, Parametric vibrations of cylindrical shells with a viscoelastic core, *Polymer Mechanics* 11 (5) (1975) 718–725.
[53] O.B. Kachaenko, L.S. Pal'ko, N.A. Shul'ga, Acoustic wave diffraction by an elastic cylindrical shell with viscous filling, *Soviet Applied Mechanics (English Translation of Prikladnaya Mekhanika)* 25 (7) (1990) 662–667.
[54] C. Jen, C. Neron, A. Miri, H. Sodab, A. Ohno, A. McLean, Fabrication and characterization of continuously cast clad metallic buffer rods, *Journal of the Acoustical society of America* 91 (1992) 3565–3570.
[55] W.W. King, C.J. Aloisio Jr., Thermomechanical mechanism for delamination of polymer coatings from optical fibers, *Journal of Electronic Packaging, Transactions of the ASME* 119 (2) (1997) 133–136.
[56] R.N. Thurston, Elastic waves in rods and clad rods, *Journal of the Acoustical Society of America* 64 (1) (1978) 1–37.
[57] R. Parnes, Torsional dispersion relations of waves in an infinitely long clad cylindrical rod, *Journal of the Acoustical Society of America* 71 (6) (1982) 1347–1351.
[58] K.D. Bennett, S.J. Hanna, R.O. Claus, Monitoring of stain in layered media using clad rod acoustic waveguides, *Ultrasonic Symposium Proceedings* (1985) 1064–1067.
[59] J.A. Simmons, E. Drescher-Krasicka, H.N.G. Wadle, Leaky axisymmetric modes in infinite clad rods. I,, *Journal of the Acoustical society of America* 92 (1992) 1061–1090.
[60] A.D. Pierce, *Acoustics; An Introduction to its Physical Principles and Applications*, American Institute of Physics, New York, 1991.
[61] M. Abramovitz, I.A. Stegun, *Handbook of Mathematical Functions*, National Bureau of Standards, Washington, DC, 1964.
[62] R.L. Willis, L. Wu, Y.H. Berthelot, Determination of the complex young's and shear dynamic moduli of viscoelastic materials, *Journal of the Acoustical Society of America* 109 (2) (2001) 1–11.

[63] K.S. Cole, R.H. Cole, Dispersion and absorption in dielectrics, *Journal of Chemical Physics* 9 (1941) 341–351.
[64] D.W. Davidson, R.H. Cole, Dielectric relaxation in glycerine, *Journal of Chemical Physics* 18 (1950) 1417.
[65] S. Havriliak, S. Negami, A complex plane analysis of α-dispersions in some polymer systems, in transitions and relaxations in polymers, *Journal of Polymer Science Part C* 14 (1966) 99–117.
[66] J. Vollmann, J. Dual, High-resolution analysis of the complex wave spectrum in a cylindrical shell containing a viscoelastic medium, Part I. Theory and numerical results, *Journal of the Acoustical Society of America* 102 (1997) 896–908.
[67] J.D. Achenbach, *Wave Propagation in Elastic Solids*, North-Holland, New York, 1976.
[68] J.A. Stratton, *Electromagnetic Theory*, McGraw-Hill, New York, 1941.
[69] V.V. Varadan, Y. Ma, V.K. Varadan, A. Lakhtakia, Scattering of waves by spheres and cylinders, in: V.V. Varadan, A. Lakhtakia, V.K. Varadan (Eds.), *Field Representations and Introduction to Scattering*, North-Holland, Amsterdam, 1990, pp. 211–322.
[70] E.B. Danila, J.M. Conoir, P. Pareige, J.L. Izbicki, Multichannel resonant scattering theory applied to the acoustic scattering by an eccentric elastic cylindrical shell immersed in a fluid, *Wave Motion* 28 (1998) 297–318.
[71] S.M. Hasheminejad, M. Rajabi, Acoustic resonance scattering from a submerged functionally graded cylindrical shell, *Journal of Sound and Vibration* 302 (2007) 208–228.